PNAS RESEARCH ARTICLE | SYSTEMS BIOLOGY OPEN ACCESS

Single cell–resolved cellular, transcriptional, and epigenetic changes in mouse T cell populations linked to age-associated immune decline

Jing He[a,1], Elena Burova[a,1], Chandrika Taduriyasas[a], Min Ni[a], Christina Adler[a], Yi Wei[a], Nicole Negron[a], Kun Xiong[a], Yu Bai[a], Tea Shavlakadze[a], Ella Ioffe[b], John C. Lin[a], Adolfo Ferrando[a,2], and David J. Glass[a,2]

Contributed by David J. Glass; received December 20, 2024; accepted February 24, 2025; reviewed by Iannis Aifantis and Pura Muñoz-Canoves

Splenic T cells are pivotal to the immune system, yet their function deteriorates with age. To elucidate the specific aspects of T cell biology affected by aging, we conducted a comprehensive multi–time point single-cell RNA sequencing study, complemented by single-cell Assay for Transposase Accessible Chromatin (ATAC) sequencing and single-cell T cell repertoire (TCR) sequencing on splenic T cells from mice across 10 different age groups. This map of age-related changes in the distribution of T cell lineages and functional states reveals broad changes in T cell function and composition, including a prominent enrichment of Gzmk+ T cells in aged mice, encompassing both CD4+ and CD8+ T cell subsets. Notably, there is a marked decrease in TCR diversity across specific T cell populations in aged mice. We identified key pathways that may underlie the perturbation of T cell functions with aging, supporting cytotoxic T cell clonal expansion with age. This study provides insights into the aging process of splenic T cells and also highlights potential targets for therapeutic intervention to enhance immune function in the elderly. The dataset should serve as a resource for further research into age-related immune dysfunction and for identifying potential therapeutic strategies.

aging | T cells | aging gene signature | single-cell RNA | granzyme K

Aging is associated with a decline in immune function, and older individuals have an increased susceptibility to infection, a need for increased vaccine dosages to achieve neutralizing antibody titers, a higher incidence of autoimmune diseases, and a greater prevalence of cancer—partly due to diminished immune surveillance (1, 2). Therapeutically, inhibition of mammalian Target of Rapamycin Complex 1 signaling with rapamycin or its analogs (3) has been explored even in humans to counteract immune senescence and enhance vaccine responses (4–6). However, effective strategies for reversal of age-associated immune decline remain a major unmet need.

Given this context, a critical question arises: "How does aging affect immune cells at the molecular level?" Several studies have addressed this question in various contexts. For instance, Young et al. (7) reported an expansion of memory CD8+ T cells with age, and identified 29 candidate Alzheimer's disease genes in T cells. In a separate study (8), a single-cell transcriptomic analysis of CD4+ T regulatory (Treg) cells from mice aged 3, 18, and 24 mo revealed distinct clusters of Treg cells, including an increase in proinflammatory cells and a reduction in precursor cells. Additionally, increased senescence in T cells, particularly in CD8+ T cell populations, is found by monitoring beta-galactosidase levels of human donors in their 60s (9).

Previous studies expanded the understanding of age-associated changes in T cells in rodents and humans (10–13); several highlighted the decline in T cell function and increased susceptibility to infections, autoimmunity, and cancer with age (14–16) and discussed thymic involution and the global shift from naive to memory T cell phenotypes (17–19).

Recent analyses revealed the presence of distinct subpopulations of age-associated granzyme K (Gzmk) expressing CD4+ T cells that accumulate in aged mice (20); another study described clonal cytotoxic Gzmk+ CD8+ T cells as a hallmark of inflammaging in mice and humans (21). Furthermore, naive CD8+ T and Naive Treg cells in human peripheral blood decrease with age, while Th1/Th17 CD4+ memory cells increase with age (22).

Building on this prior work, we recognized the importance of conducting a study that included multiple time points along the mouse lifespan, using single-cell RNA-seq of both CD4+ and CD8+ T cells with a large sample size and deep sequencing. This approach aims to provide a comprehensive view of aging-associated changes in T cells, capturing

Significance

Aging impacts the immune system, including the function of splenic T cells, which are crucial for immune defense. Our study used advanced single-cell sequencing techniques to map changes in T cell biology across the lifespan of mice. We identified significant shifts in T cell types, including an increase in Gzmk+ T cells and a decrease in T cell diversity in aged mice. These findings further reveal changes in key pathways that may drive accelerated T cell dysfunction, suggesting potential targets for boosting immune function in the elderly. Our dataset serves as a resource for future research on immune aging and rejuvenation strategies.

Author affiliations: [a]Regeneron Pharmaceuticals, Tarrytown, NY 10591; and [b]Preclinical and Early Development, Cullinan Therapeutics, Cambridge, MA 02142

Author contributions: E.B., K.X., Y.B., T.S., E.I., and D.J.G. designed research; E.B., C.T., M.N., C.A., and N.N. performed research; J.H., M.N., Y.W., J.C.L., A.F., and D.J.G. analyzed data; K.X. and Y.B. conducted the pathway enrichment analysis; and J.H., E.B., A.F., and D.J.G. wrote the paper.

Reviewers: I.A., NYU School of Medicine; and P.M.-C., Altos Labs Inc.

Competing interest statement: The authors were all employees of Regeneron Pharmaceuticals when this work was performed. Most hold stock or stock options exceeding $5000 in value.

[1]J.H. and E.B. contributed equally to this work.

[2]To whom correspondence may be addressed. Email: adolfo.ferrando@regeneron.com or david.glass@regeneron.com.

This article contains supporting information online at https://www.pnas.org/lookup/suppl/doi:10.1073/pnas.2425992122/-/DCSupplemental.

Published March 31, 2025.

early-, mid-, and late-lifespan alterations to address questions of "potential cause versus effect." Furthermore, we integrated single-cell RNA sequencing (scRNA-seq) with single-cell ATAC sequencing (scATAC-seq) and single-cell TCR sequencing (scTCR-seq) to correlate age-related gene expression changes with potentially causal epigenetic alterations, and the resultant perturbation in T cell repertoire (TCR) clonality (23).

Results

scRNA-seq Mapping of T Cell Population Across the Mouse Lifetime Reveals New Subpopulations. To assess the effects of young and aged host environments on T cells, we analyzed splenic T cells from healthy male mice of 10 age groups (10 to 117 wk) with at least eight mice per group. CD3+ T cells were enriched to over 95% (*SI Appendix*, Fig. S1*A*), and 301,674 cells were isolated for single-cell transcriptomics (scRNA-seq) and TCR sequencing (scTCR-seq) using the 10× Genomics platform (Fig. 1*A*) (24, 25). Additionally, we profiled chromatin accessibility in splenic CD3+ T cells from young (24 wk), adult (48 wk), aged (84 wk), and old (108 wk) mice using scATAC-seq (Fig. 1*A*).

From the scRNA-seq analysis, 291,860 cells passed quality control criteria, with 94% identified as T cells based on Ptprc, Cd3e, and Cd3d expression (*SI Appendix*, Fig. S1*B*). Unsupervised clustering via Scanpy (26) (*Materials and Methods*) revealed 20 distinct cell clusters (Fig. 1*B*) corresponding to functionally diverse T cell populations (27). These clusters included 11 CD8+ T cell clusters (C0-C10), 7 CD4+ T cell clusters (C12-C18), 1 Natural Killer T (NKT) cell cluster (C19), and a Gzmk+ T cell cluster with both CD4+ and CD8+ T cells (C11).

Notably, subclustering of cluster C11 revealed nine subclusters of mixed CD4+ and CD8+ T cells with varying Gzmk expression levels (Fig. 1*C*). This indicates that cytotoxic signatures may define these cells more than their respective CD4+ or CD8+ identities together in one Gzmk+ cluster. The highest Gzmk expression was observed in CD4+ T cells subcluster 3. We designated Gzmk+ CD8+ T cells as cluster C11a and Gzmk+ CD4+ T cells as cluster C11b.

Cluster C19 comprised less than 2.7% of all cells, expressing Cd3e and Cd3d along with high levels of NK cell lineage marker Klrb1c and NK-gene complex marker Klrk1 (*SI Appendix*, Fig. S1*C*) indicative of NKT cells that copurified with T cells.

CD8+ T Cell Clusters from scRNA-seq. Analyzing CD8+ T cells identified 12 distinct clusters, including five Naive/Stem cells clusters (Naive C0, Naive.Early Activation C1, Naive.Isg15 C2, Naive.Stem 1 C3, and Naive.Stem 2 C4), 2 Effector memory clusters (T Effector memory C5, Tissue-resident memory C6), a Central Memory cluster (C7), an Effector cell cluster (C8), a Terminal Effector cell cluster (C9), a Proliferating cells cluster (C10) and a Gzmk+ cluster (C11a). Each cluster exhibits unique gene expression patterns characteristics of specific CD8+ T cell states (Fig. 1*D* and *SI Appendix*, Fig. S1 *D–F*).

Naive CD8+ T cell cluster C0, C1, and C2 displayed high expression of naive markers such as Lef1, Dapl1, Igfbp4, and Sell (L-selectin, CD62L) (Fig. 1*D* and *SI Appendix*, Fig. S1*D*). The Naive Early Activation Cluster C1 expresses genes like Junb/d, Dusp1/10, Klf2/6, Vps37b, Ccr7, and Nr4a1, which are involved in IL7R regulation and T cell signaling (*SI Appendix*, Fig. S1*E*) (28–31). The Naive.Isg15 cluster C2 overexpresses type 1 interferon (IFN) response genes (Isg15, Ifit3, Ifit203, Irf7), indicating active IFN signaling (Fig. 1*D* and *SI Appendix*, Fig. S1*E*) (32, 33). Naive.Stem1 (C3) and Naïve.Stem2 (C4) clusters also express naive markers including Sell, Lef1, Ccr7, but show elevated Tcf7 levels, suggesting self-renewal potential without distinct transcriptional features (*SI Appendix*, Fig. S1 *D* and *F*) (34).

We identified three major memory CD8+ T cell clusters. Cluster C5 (T Effector Memory) circulates through peripheral tissues via the vasculature and expresses Cd44, Eomes, Bcl2, and Il7r (*SI Appendix*, Fig. S1*D*). Central memory T cells in cluster C7 circulate between blood, lymphoid, and nonlymphoid sites and exhibit a higher Ccr7 level compared to TEM cells. Cluster C6 represents tissue-resident memory T cells (TEM.Tissue Resident), which shares markers such as Cd44,

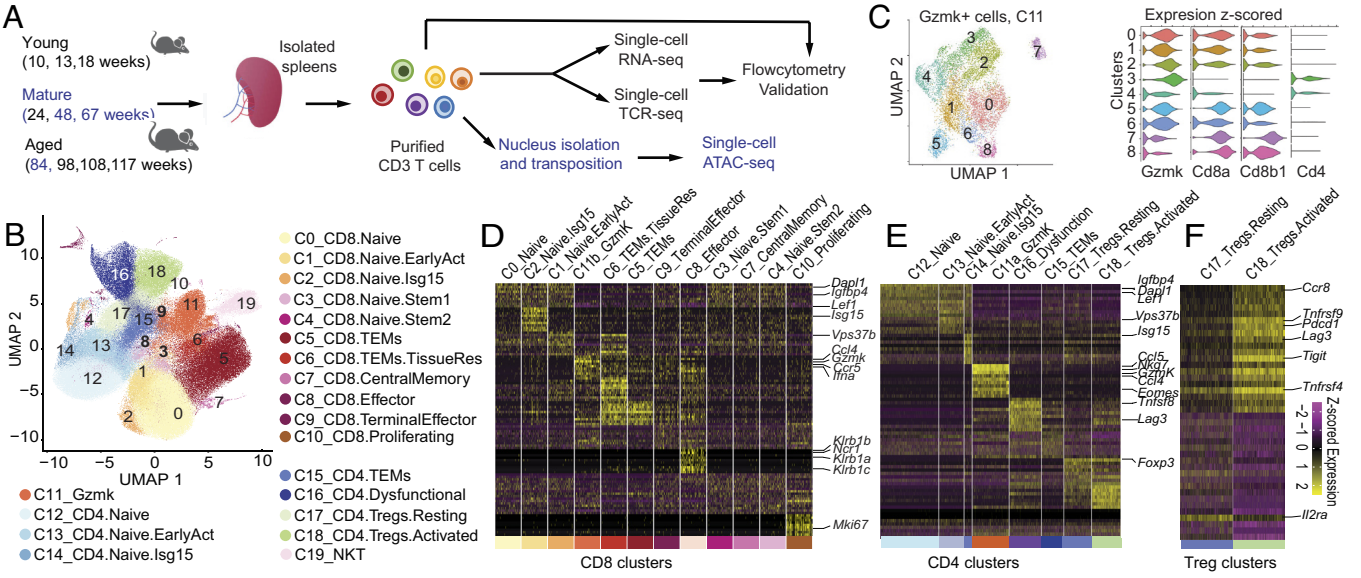

Fig. 1. Single-cell transcriptional profiling of aging mouse splenic T cells. (*A*) Experimental flow chart. Mouse splenocytes were harvested from 10 different age groups. CD3+ T cells were purified. CD3+ T cells were barcoded using 10× platform and profiled by scRNA-seq and scTCR-seq. Flow cytometry was used to evaluate age-associated functional changes. Mouse T cell scATAC-seq was done on 4 age groups. (*B*) UMAP of 20 annotated CD3+ T cell clusters. (*C*) Heterogeneity of Gzmk+ cells. (*Left*) UMAP of Gzmk+ CD3+ T cells (C11), a mixture of CD4+ and CD8+ T cells. (*Right*) Z-scored expression of marker genes across nine subsets (*D–F*). Heatmaps of marker gene expression z-scores across different populations of (*D*) CD8+ T, (*E*) CD4+ T, and (*F*) CD4+ Tregs cells. (*D* and *E*) Genes shown were upregulated significantly [ln(fold change) > 0.4, combined p < 10E−3) in at least one subset compared to all other cells. Genes were ordered by significance and associated with the subset with higher detection rates. (*F*) Genes shown were upregulated significantly in activated Tregs compared to resting Tregs.

Eomes, Bcl2, and Il7r with TEM but also constitutively expresses early activation marker Cd69 (35), which promotes tissue retention by inhibiting S1P-mediated egress (*SI Appendix*, Fig. S1 *D* and *F*) (36).

Two distinct Effector cell clusters were identified: Effector (C8) and Terminal effector (C9). Both clusters correlate with a terminal exhausted T cell signature (37), with the Terminal Effector cluster showing high killer cell lectin-like receptor (Klrg1) expression (38) alongside Eomes and Cd44 expression (*SI Appendix*, Fig. S1*D*). The Effector cluster expresses cytotoxic function-related transcripts such as Klrb1a, Klrb1b, Klrb1c, Krb1f, KlrK1, Klrc1, Klre1 (Fig. 1*D* and *SI Appendix*, Fig. S1*F*), and cytotoxic immune response–related genes such as Ncr1, Xcl1.

Cluster C10 exhibited high expression of Mki67 (Fig. 1*D* and *SI Appendix*, Fig. S1F) and correlation with proliferating signature (*SI Appendix*, Fig. S1*G*) (37), along with genes associated with cell division (Cdca8, Cdc20, Cdca3) and mitotic chromosome segregation (Cenpf, Cenpe)(*SI Appendix*, Fig. S1*F*). This population was small across all age groups analyzed, reflecting low CD8+ T proliferation levels. Cytotoxic Gzmk+ cluster (C11a) expresses multiple cytotoxic effector T cell transcripts, including Gzmk and Ifnγ, as well as the chemokine (C–C motif) ligand Ccl4 and its receptor Ccr5 (21) (Fig. 1*D*).

CD4$^+$T Cell Clusters from scRNA-seq. In addition to CD8+ T cell populations, we identified 8 distinct CD4+ T cell clusters (Fig. 1 *E* and *F* and *SI Appendix*, Fig. S2*A*): three naive clusters [Naive C12, Naive.Early Activation (C13) and Naïve.Isg15 (C14)]; T Effector Memory cluster (C15); Dysfunctional cluster (C16); 2 Treg clusters [Resting Tregs (C17) and Activated Tregs (C18)]; and a Gzmk+ cluster (C11b). Naive clusters express Lef1, Sell, Igfbp4, and Ccr7 (Fig. 1*E*) (39). Compared to Naive cluster C12, the Naive.Early activation cluster (C13) shows elevated expression of immediate-early TCR signal strength indicator (40) Nr4a1 which encodes Nur77, along with Junb, Vps37b, Klf2, Etg1, and Anrc1 (*SI Appendix*, Fig. S2*A* and *SI Appendix*, Fig. S2 *B*, *Left*). Naïve.Isg15 cluster expresses type I IFN response genes including Isg15, Isg20, Ifit1, Ifit3, and Ifit203 (*SI Appendix*, Fig. S2*A* and *SI Appendix*, Fig. S2 *B*, *Right*).

Cluster C15 (TEM) expresses S100a4 (41), Cd40lg (CD40 ligand), and the IL7 receptor Il7r (*SI Appendix*, Fig. S2*A*). In contrast, cluster C16 (CD4.Dysfunctional) shows elevated Tnfsf8, Lag3, S100a6, Tbc1d4 expression (*SI Appendix*, Fig. S2*A*) (42). The CD4.Gzmk cluster (C11b) overexpresses cytotoxic CD4+ T cell markers in cancer and viral infections (43, 44), including Gzmk, Ccl4, Eomes, Ctl2a, and Nkg7 (*SI Appendix*, Fig. S2 *A* and *D*).

Treg populations, marked by Foxp3 expression (*SI Appendix*, Fig. S2*E*), displayed distinct activation states. Activated Tregs (C18) expressed elevated levels of Tnfrsf9—a marker of antigen-experienced and functional Tregs (45); Tnfrsf4 and Ccr8—markers of active immunosuppressive Tregs (46); and Pdcd1, Lag3, and Tigit—immune-suppressive receptors genes (Fig. 1*F* and *SI Appendix*, Fig. S2*K*). In contrast, Resting Tregs (C17) exhibited higher Il2ra (CD25) expression without activation markers (*SI Appendix*, Fig. S2*K*).

The CD4+ T clusters showed strong correlation (Spearman correlation coefficients 0.928 to 0.944) (*SI Appendix*, Fig. S2*F*) with previously described clusters in aged mice (20), while revealing a distinct Naive.Early activation (C13) cluster.

This analysis revealed a diverse landscape of 20 T cell populations, highlighting significant heterogeneity within the CD8+ and CD4+ T cell compartments, emphasizing the complexity of T cell development and differentiation in response to aging.

T Cell Cluster Specific Dynamics Associated with Aging. Identification of T cell subpopulations is vital to understanding the transcriptional and epigenetic mechanisms that govern T cell function and adaptation during aging. By characterizing these populations throughout their lifespan, we aim to reveal trends in their dynamics, focusing on age-related changes in composition and functional capacity, as well as the implications for immune senescence and age-associated diseases.

Previous studies have demonstrated that age-related declines in immune function in mice are associated with both quantitative and qualitative changes in T cell populations. Specifically, aged mice show a reduction in peripheral naive cells (11, 47, 48). In our analysis, we observed a significant decrease in the total T cell reservoir in the spleens of aged mice; however, the distribution of CD4+ T cells and CD8+ T cells, as well as B cell populations, remained unchanged with age, as assessed by flow cytometry (*SI Appendix*, Fig. S3*A*).

To investigate T cell subsets dynamics during aging, we categorized mice into three age groups: young (10, 13, and 18 wk), mature (24, 48, and 67 wk), and aged (84, 98, 108, and 117 wk) (Fig. 2*A*). Based on the distribution of cell populations across timepoints in our scRNA-seq data, the transition from 24 to 48 wk of age and then from 67 to 84 wk of age seems to represent inflection points. Based on these observations we propose that mice younger than 24 wk may be considered "young" in terms of T cells, 48 to 67 wk old are considered middle aged, and animals older than 67 wk are considered aged. Young mice had higher numbers of naive T cells. In contrast, aged mice exhibited an increased prevalence of dysfunctional/effector memory T cells, Gzmk+ cells, and activated Tregs populations.

We employed the Mann–Kendall trend test to quantify the aging trends of each T cell cluster (*SI Appendix*, Table S3). Notably, the Gzmk+ cluster C11 (Tau = 0.73, $P = 0.004$), CD8+ Effector Memory cells (C5) (Tau = 0.78, $P = 0.002$), CD8+ Tissue Resident (C8) (Tau = 0.73, $P = 0.004$) and activated CD4+ Tregs (Tau = 0.73, $P = 0.004$) exhibited significant increasing trends. In contrast, the most pronounced decreasing trends were found in CD4+ Naive Early Activation cells (C13) (Tau = −0.73, $P = 0.007$) and NKT cells (C19) (Tau = −0.73, $P = 0.004$) (Fig. 2*B*).

Comparative analysis of CD8+ and CD4+ T cell clusters revealed significant age-related changes in immune population distribution, as shown in waterfall plots in Fig. 2*B* and *SI Appendix*, Fig. S2 *H–J*. Notably, aged mice exhibited a decrease in naïve CD8+ T cells (CD8.Naive, CD8.Naive.Early Activation, and CD8.Naive.Isg15) as well as naive CD4+ T cells (CD4.Naive, CD4.Naive.Early Activation, and CD4.Naive.Isg15) compared to younger mice. In contrast, naive/stem-like CD8+ T cell populations (CD8.Naive.Stem1 and CD8.Naive.Stem2) and proliferating CD8+ T cells (CD8.Proliferating) remained consistently represented across age groups.

As naive T cell populations decline with age, there was a notable increase in CD8+ and CD4+ effector/memory T cells (including CD8.TEM, CD8.Tissue resident, CD8.Terminal effector, CD4.TEM, and CD4.Dysfunctional) in aged mice. Furthermore, the number of CD8.Gzmk+/CD4.Gzmk+ cells (C11) significantly expanded in aged mice, representing the fastest-growing cluster (*SI Appendix*, Fig. S2*J*). Activated Tregs also became more prevalent in older mice, while resting Tregs maintained similar proportions across age groups.

The size of cell clusters in aged mice (108 and 117 wk of age) exhibited greater variability compared to younger mice, highlighting increased heterogeneity in immune function with age.

Orthogonal analysis of dynamic changes in T cell populations using flow cytometry in an independent cohort of young and aged

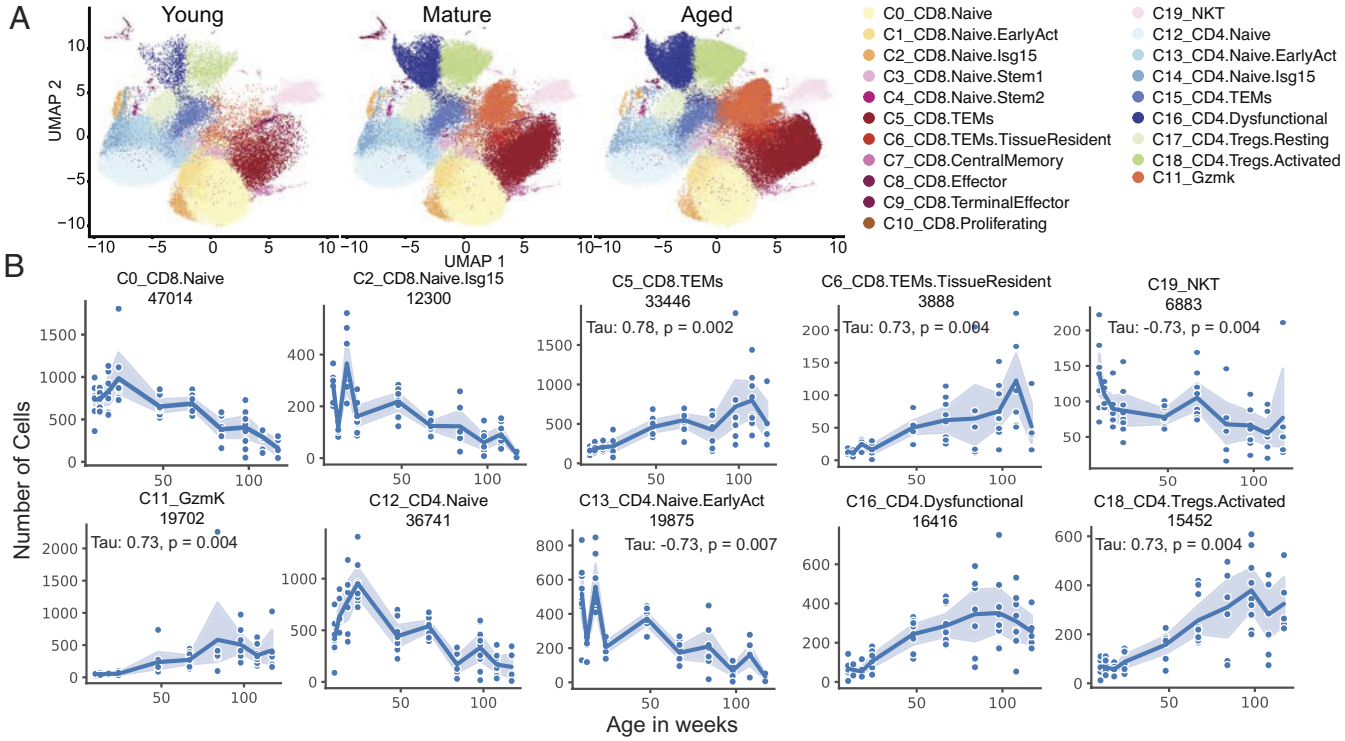

Fig. 2. Age-associated alterations in splenic T cell populations in mice. (*A*) UMAP projections of CD3+ T cell clusters separated by young, mature, and aged group. (*B*) Age-related shifts in T cell single-set defined cluster distribution with age. Absolute numbers of each T cell subset as a function of age analyzed out of total sequenced cells in a subset.

mice revealed a reduced frequency of naive cells (CD44-CD62L+) and an increase in effector memory cells (CD44+CD62L–) and central memory cells (CD44+CD62L+) within both the CD4+ and CD8+ T cell compartments of aged mice (*SI Appendix*, Fig. S3*B*). These results align with our scRNA-seq data and prior studies (20, 49). Furthermore, we noted a decrease in the absolute number of total CD4+ T cells per gram of spleen in aged (100 wk) compared to young (8 wk) mice (*SI Appendix*, Fig. S3*C*).

Flow cytometry gating was performed for CD4.Gzmk+ cytotoxic T cells (CD4+EOMES+CCL5+) (*SI Appendix*, Fig. S3 *D*, *Top*), CD4. Exhausted T cells (defined as CD4+PD1+CD62L–Foxp3–EOMES–CCL5–) and CD4.TEMs (defined as CD4+PD-1–CD62L– Foxp3–EOMES–CCL5–) (*SI Appendix*, Fig. S3 *D*, *Bottom*), following the methodology outlined in ref. 20. Our analysis revealed that the numbers of cytotoxic CD4+ T and dysfunctional CD4+ T cells increased with age, while CD4+ TEM population showed a trend toward increased numbers with age albeit with high variability, and an apparent drop in frequency at our latest age week 117 (*SI Appendix*, Fig. S2 *G* and *H*).

Activated Tregs can be distinguished from resting Tregs by CD81 marker expression in flow cytometry (20) (*SI Appendix*, Fig. S3*E*). In aged mice, activated Tregs (aTregs, CD4+FoxP3+ CD81+) were significantly more prevalent, while resting Tregs (rTregs, CD4+FoxP3+CD81–) were similarly represented in both young and aged mice (*SI Appendix*, Fig. S3*C*). Furthermore, activated Tregs exhibited higher expression of PD-1, LAG-3, TIGIT, and TIM-3 compared to resting Tregs, with additional upregulation of PD-1, LAG-3, and TIGIT observed in the aTreg population of aged mice (*SI Appendix*, Fig. S3*F*).

Flow cytometry analysis revealed that age-related changes in CD4+ T cell populations align closely with the scRNA-seq data. We observed dynamic shifts in splenic T cell populations, including increased frequencies of activated Tregs and CD4+ and CD8+ T effector/memory subsets. Notably, the most significant expansions occurred in the Gzmk+ T cell and dysfunctional T cell subsets.

To assess the impact of aging on T cell functionality, we examined the activation responses of CD8+ T cells isolated from the spleens of 24-wk-old and 98-wk-old mice. These cells were stimulated in vitro using anti-CD3 and anti-CD28 antibodies, and cytokine production was analyzed after 24 h. The results showed that CD8+ T cells from aged mice produced significantly higher levels of IFNγ and GzmB compared to cells from younger mice, while IL-2 production remained unchanged (*SI Appendix*, Fig. S3*G*).

In young mice, both PD1high and PD1low cells produced IFNγ and GzmB. However, aged mice exhibited reduced production of these cytokines in PD1high CD8+ T cells compared to PD1low CD8+ T cells, indicating diminished cytokine secretion capacity in dysfunctional CD44+ PD1high CD8+ T cells (*SI Appendix*, Fig. S3*H*). Notably, aged CD8+ T cells still produced GzmB efficiently and secreted inflammatory chemokines CCL3, CCL4, and CCL5 (*SI Appendix*, Fig. S3*I*), characteristic of effector cells responding to pathogens and vaccines.

These results indicate that aging correlates with heightened production of inflammatory and cytotoxic cytokines, reflecting changes that promote proinflammatory T cell responses.

TCR Repertoire Diversity and Clonality Changes with age. Thymic involution, marked by reduced size and output, correlates with decreased TCR diversity in aging (50, 51). The murine thymus peaks at 4 wk (52), declining to 50% of its mass at 16 wk and retaining less than 5% of its cellularity thereafter (52–55). Aged mice typically show diminished TCR diversity due to this involution (11, 47, 48), although some evidence suggests partial thymic functionality persists in older mice (19). Consequently, reduced thymic output leads to fewer newly generated naive T cells in the periphery. This, coupled with the clonal expansion

of memory T cells, results in increased TCR clonality in aged mice (56, 57).

To investigate the impact of aging on TCR clonality, we quantified TCR clone sizes using unique TCR sequences from scRNA-seq data across T cell populations in mice of varying ages. The analysis revealed an increase in TCR clone size, particularly in lymphocyte clusters such as CD4.Activated Tregs, CD8.TEMs, and CD8.Gzmk populations in aged mice (Figs. 1*B* and 3*A*).

We then assessed T cell clonality using the Gini coefficient, which measures population imbalance (Fig. 3*B*). A significant increase in clonality was noted at 13 wk, likely due to heightened antigen-driven clonal proliferation during this early stage. In adult mice, clonality generally increased from 18 to 117 wk of age, particularly within the CD8.Gzmk subset. Notably, both CD4.Gzmk+ T cells (C11b) and CD8.Gzmk+ T cells (C11a) exhibited increased clonality (Fig. 3*C*). Additionally, CD8.TEMS (C5), CD8.TEMS. Tissue Resident (C6), CD4.Dysfunctional T cells (C16), and activated Tregs (C18) also demonstrated age-related increases in clonality. In contrast, Naive CD8+ (C0, C1, C2) and naive CD4+ (C12, C13, C14) T cell clusters showed lower levels of TCR clonality, as expected.

We next analyzed TCR repertoires from aged mice and identified the top 10 most expanded T cell clones based on TCRα and/or TCRβ chain proportions. We traced these clones across different ages and individual mice, revealing that all top clones originated from aged animals: one mouse at 48 wk (#7), five at 84 wk (#2–#6), one at 98 wk (#1), and two at 117 wk (#8 and #9) (*SI Appendix*, Fig. S3*J*). Notably, the age-associated TCR clones were largely distinct among individual mice, with 5 of the 10 top clones unique to specific mice, while the remainder were shared between pairs of mice in the same age group.

Therefore, T cells undergo significant clonal expansion in aged mice, particularly Gzmk+ cells within both CD8+ and CD4+ compartments. The substantial expansion of splenic Gzmk+ CD4+ and CD8+ T cells with age highlights their role as key drivers of the restricted TCR repertoire in aging.

Epigenomic Landscape of Splenic T Cells in Aging Mice. T cell development, activation, and function are regulated by transcriptional networks that convert extracellular signals, such as antigen-MHC TCR engagement and cytokine signaling, into gene expression changes. To investigate the regulatory mechanisms underlying age-related T cell alterations, we profiled the chromatin accessibility of purified splenic T cells from mice aged 24, 48, 84, and 108 wk using scATAC-seq (ATAC with high-throughput sequencing) (Fig. 1*A*). We analyzed samples from eight mice per age group, yielding a total of 36,074 CD4+ and 24,860 CD8+ T cells that passed quality control criteria (Fig. 4*A*). While no significant changes were observed in the ATAC-seq profiles of CD4+ or CD8+ T cells across age groups (*SI Appendix*, Fig. S4*A*), individual analyses revealed a slight trend of decreased CD8+ T cells alongside an increase in CD4+ T cell populations with aging (*SI Appendix*, Fig. S4*B*).

Chromatin accessibility peaks identified by ATAC-seq indicate transcriptional potential and serve as markers for lineage and function. Using these data, we identified eight distinct CD4+ T cell clusters with varying chromatin states (Fig. 4*B*): Naive (C5), Memory (C4, Mem), Effector Memory (C3, Eff. Mem), Cytotoxic (C2, Cyto), Activated (C1, Act), Treg (C8, Tregs), Type 1 T Helper (C6, Th1), and Type 17 T Helper (C7, Th17). These clusters were named based on signature genes with differential accessibility, gene activity scores (Fig. 4*C* and *SI Appendix*, Fig. S5 *A* and *C*), and transcription factor motif enrichment in accessible chromatin regions (Fig. 4*C*).

Several genes exhibit different accessibility patterns in specific T cell clusters. For instance, Il17α is accessible in Th17 cells (Fig. 4*C*), Pdcd1 in activated and cytotoxic CD4+ T cells (Fig. 4*C*), Gzmk in cytotoxic CD4+ T cells (Fig. 4*C*), and Foxp3 in Tregs (Fig. 4*C*). Additionally, Lef1 is prominent in naive CD4+ T cells, Ifng in cytotoxic and Th1 CD4+ T cells, and Il-2 in memory, Th1, and Th17 CD4+ T cells (*SI Appendix*, Fig. S5 *A* and *C*). Gene activity scores derived from chromatin accessibility highlight Sell in naïve CD4+ clusters, Foxp3 in Tregs, and Gzmk in cytotoxic T cells, alongside established markers such as IL-17α and RORγ, which is crucial for Th17 cell specification (Fig. 4*E* and *SI Appendix*, Fig. S5 *A* and *B*).

Differential peaks based on chromatin accessibility revealed that the Naive CD4+ T cell cluster exhibits the most distinct profile. Notably, these naive CD4+ specific peaks are also moderately accessible in Memory and Effector Memory CD4+ T cells (Eff.Mem) (*SI Appendix*, Fig. S4*E*). Differential peaks were also observed in Effector Memory CD4+ T cells, as well as in Th1 and cytotoxic CD4+ T cells, which share a core set of peaks with varying accessibility levels. Similarly, activated CD4+ T cells and Tregs possess a unique set of accessible chromatin regions, characterized by differing levels of accessibility.

We evaluated the chromatin-inferred activity of established marker genes in CD4+ T cell subtypes. Notably, we found elevated activity levels for Lef1 and Sox4 in naive CD4 T cells; Il21, Tnfsf8, and Ccr6 in Activated CD4; Foxp3 and Klrc1 in Tregs; Il17a, Sxcr6, and S100a4 in Th17; Rora, Ccl5, and Ctla2a in Effector memory CD4; and Ifnγ, Il13, Gzmk, Gzmb, Eomes, and Tbx21

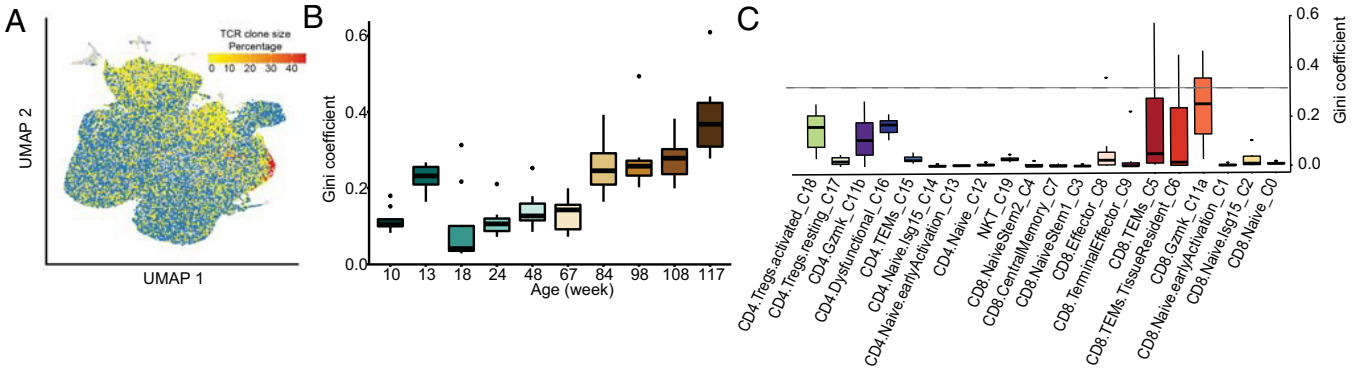

Fig. 3. TCR repertoire diversity decreases in aging splenic CD3$^+$ T cells. (*A*) TCR clones are shown on UMAP projection of all CD3+ T cells isolated from spleens. (*B*) Paired single-cell TCRα/β repertoire (measured as Gini coefficient) per T cells across different age groups. (*C*) Low TCR diversity of CD4.Gzmk and CD8.Gzmk and CD8.TEMs cells. Paired single-cell TCR α/β repertoire (measured as Gini coefficient) per T cells across different CD3-positive clusters. Data are mean ± SEM for all mice (n = 83) of all 10 age groups.

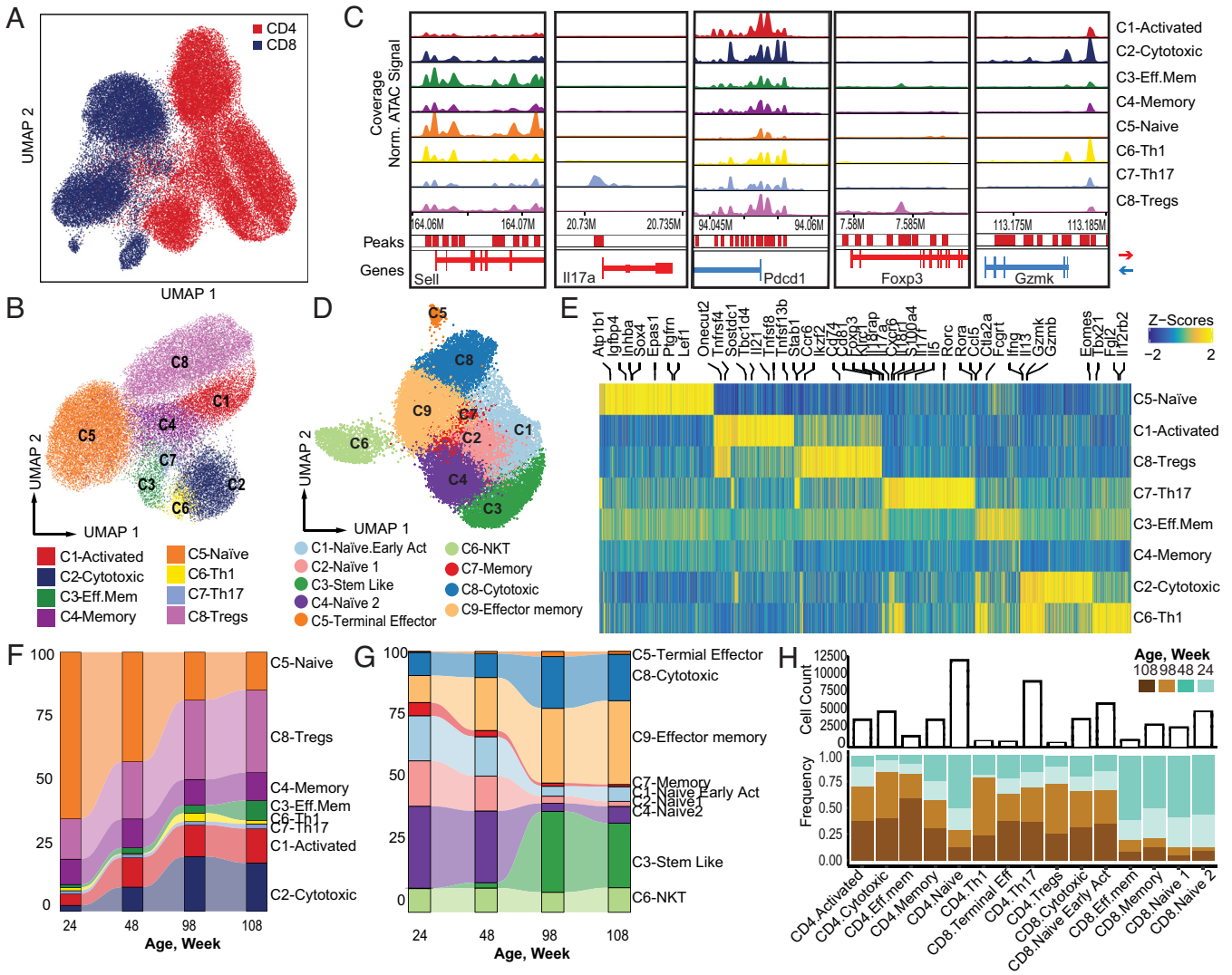

Fig. 4. Single-cell analysis of chromatin accessibility associated with age in mouse splenic T cells. (*A*) scATAC-seq clusters of T cells isolated from the spleen (60,934 cells) from young and aged C57Bl/6J male mice (pool of n = 8 per age group; mice of 24, 48, 84, and 108 wk old). Shown is CD4+ T cell and CD8+ T cell cluster composition. (*B*) UMAP projection of annotated clusters of CD4+ T cells. (*C*) Genome tracks of aggregate scATAC-seq data visualization of the locus Sell, Il17a, FoxP3, Pdcd1, Gzmk, clustered as indicated in *B*. (*D*) UMAP projection of annotated clusters of CD8+ T cells. Gene activity of selected T cell markers in CD4+ T clusters. Color gradient indicates z-scored gene activity level (yellow represents high; blue represents low). (*E*) Top peak/gene score per clusters. Scores are column-wise z-scored. Peak score represents chromatin accessibility of a given peak (each row). Gene score (each row) represents the aggregated score of all peaks of a given gene after normalization. (*F* and *G*) Representative plots showing the frequencies dynamics of ATAC-seq defined (*F*) CD4+ and (*G*) CD8+ cell clusters along aging. (*H*) Representative plots showing the frequencies and cell count of cells belonging to each of the subsets as defined by scATAC-seq of 24-, 48-, 98-, and 108-wk mice. (*H*) Representative plots showing the frequencies and cell counts of cells belonging to each of the subsets as defined by scATAC-seq of 24-, 48-, 98-, and 108-wk mice.

in Cytotoxic CD4. Additionally, we observed cluster-specific accessibility at key loci, such as Gzmk, Eomes, and Tbx21, with Cytotoxic CD4 and Th1 cells exhibiting the highest promoter accessibility (Fig. 4*E*).

Cross-comparison of transcriptional and chromatin accessibility features in CD4+ T cells demonstrates that scATAC-seq peaks align well with the transcriptional signatures of major populations identified in scRNA-seq data (*SI Appendix*, Fig. S6 *A* and *B*). Both methods consistently identified three naive CD4+ T cell populations, along with activated, memory, and cytotoxic (Gzmk) CD4+ T cell clusters (*SI Appendix*, Fig. S6*B*). Notably, some CD4+ T cell subsets were uniquely identified by scATACseq, highlighting the greater sensitivity of chromatin-based classification. For instance, we identified a CD4.Th17 cluster in scATAC-seq that was not detected in our scRNA-seq analyses (Fig. 4*B*). This Th17 CD4+ population is associated with chronic inflammation and autoimmunity (58) and showed an increase with age in our scATAC-seq analysis (Fig. 4*H*), consistent with previous findings (59).

In total, seven clusters of CD4+ T cells—CD4.Tregs, CD4. Effector Memory, CD4.Memory, CD4.Th1, CD4.Th17, CD4. Activated, and CD4.Cytotoxic—expanded in aged mice compared to young mice. Conversely, the CD4.Naive cluster contracted from 64.26% at week 24 to 14.53% at week 108 (Fig. 4 *F* and *H* and *SI Appendix*, Fig. S4*F*). Notably, the small CD4.Cytotoxic cluster increased significantly from 2.33% at week 24 to 21.17% in aged mice, while CD4.Naive cells declined with age (Fig. 4*H* and *SI Appendix*, Fig. S4*F*).

Among the total of 24,860 CD8+ T cells analyzed, we identified three distinct clusters of CD8.Naive cells: C1 (2,748 cells), C2 (4,522 cells), and C4 (2,376 cells). We also identified a CD8.Stem-like cluster (C3, 3,579 cells), characterized by Lef1+ CD44– expression and elevated Tox levels. Additionally, we recognized the following clusters: CD8.Effector Memory (C8, 5,639

cells), CD8.Cytotoxic (C9, 3,521 cells), CD8.Memory (C7, 657 cells), and a small cluster of CD8.Terminal Effector cells (C5, 261 cells) (Fig. 4*D* and *SI Appendix*, Fig. S7*A*).

The CD8 subpopulations—CD8.Naive. EarlyActivation (C1), CD8.Naive 1 (C2), CD8.Naive2 (C4), and CD8.Stem-like (C3)—exhibit distinct cluster-specific peaks and high chromatin accessibility for Ccr7 expression (*SI Appendix*, Fig. S7*A*). In contrast, the CD8.Effector memory (C8), CD8.Cytotoxic (C9), and CD8.Terminal Effector (C7) clusters share a core set of peaks with varying accessibility levels. Notably, the CD8.Terminal Effector cluster shows the highest chromatin accessibility for inflammatory and cytotoxic genes (Gzmm, Ccl9, Klrd1, Klrk1, Klrc1) compared to other CD8+ T cell populations.

To clarify the distinctions between the closely related CD8. Cytotoxic and CD8.Effector Memory cell clusters, we compared the gene activity of key markers inferred from scATAC-seq data. Our analysis revealed that CD8.Cytotoxic cells exhibit higher levels of Gzmk, while other cytotoxic molecules such as Gzmb, Gzmm, Nkg7, and inflammatory cytokines Ccl5, Ccl6, and Ccl9 are more prominent in the CD8.Effector Memory group (*SI Appendix*, Fig. S7*A*). Additionally, chromatin accessibility data indicate that the Ccr7 promoter is more accessible in CD8. Cytotoxic clusters (C8) compared to CD8.Effector Memory clusters (C9) (*SI Appendix*, Fig. S7*B*).

We observed a decline in chromatin-defined CD4.Naive, CD8. Naive, and CD8.Memory clusters across age groups, alongside an expansion of CD4.Cytotoxic, CD8.Cytotoxic, CD4.Activated, Tregs, CD8.Effector memory, and CD8.Terminal Effector clusters in aged animals compared to young mice (Fig. 4 *F*–*H*). These results align closely with our scRNA-seq findings.

Subclustering of Naive CD4+ T cells (cluster C5) revealed three distinct clusters (7, 8, and 9) (Fig. 5 *A* and *B*), indicating that naive CD4+ T cells comprise three discrete populations with varying transcriptional states. We investigated the relationships among Naive-C7, Naive-C8, and Naive-C9 using pseudotime analysis along a trajectory where Naive-C7 served as the root, Naive-C9 as an intermediate transition, and Naive-C8 as the final developmental stage. This analysis inferred the developmental stage of individual cells based on their proximity to cluster centers (Fig. 5*C*), revealing a trajectory that reflects the differentiation stages of naive CD4+ T cells from a naive state to early activation.

To investigate the transcriptional changes in naive T cells along their developmental trajectory, we aligned the cells by inferred pseudotime and analyzed associated motifs and peaks (Fig. 5*C*). Recent analyses indicate that accessible chromatin regions in naive T cells are predominantly occupied by Ets1, Runx1, and Tcf1 (60). Our data reveal that transcription factor binding motifs for Runx factors (Runx1, Runx2, Runx3) and Ets factors (Ets1, Elf1, Elf2, Elf3, Elf5, Etv2) are enriched in Naive-C7 CD4+ T cells but downregulated in Naive -C8 and Naive -C9 CD4+ T cells (Fig. 5*C*). This supports the idea that gene expression in naive T cells relies heavily on a few key transcription factor families, particularly Ets and Runx.

Additionally, Ctcf and its related factor, Ctcf-like (Ctcfl or Boris), are enriched in Naïve-C9 CD4+ T cells, while motifs for Nfat (Nfatc1, Nfatc2, Nfatc3, Nfatc4), Fos/Fosb (Fos, Fosb, Fosl1), Batf (Batf, Batf3), and Nfkb (Nfkb1, Nfkb2)—activated downstream of TCR signaling—become highly accessible in Naïve-C8 CD4+ T cells. Previous studies have shown that Batf regulates the recruitment of Ctcf to promote chromatin looping associated with lineage specific gene transcription (61). This chromatin organization is largely dependent on Ets1, which is crucial for Batf- mediated recruitment of Ctcf (61). The progressive opening of TF binding sites for Ets1, Ctcf, and Batf aligns with their cooperative role in chromatin organization during the transcriptional reprogramming associated with naive CD4+ T cell activation (62) (Fig. 5*C*).

Footprint analysis at Tcf7 binding sites in naive CD4+ T cell subpopulations (Fig. 5*D*) revealed significant changes in local chromatin accessibility associated with Tcf7, an important factor in early T cell development. Specifically, there was a marked reduction in accessibility at Tcf7 binding sites as cells transitioned from early CD4.Naive- C7 to CD4.Naive-C9 and CD4.Naive-C8, which are closer to effector/memory cells. This reduction continued in fully differentiated CD4.Memory T cells, supporting the notion that Tcf7 is dispensable for the survival of CD4+ memory T cells (63).

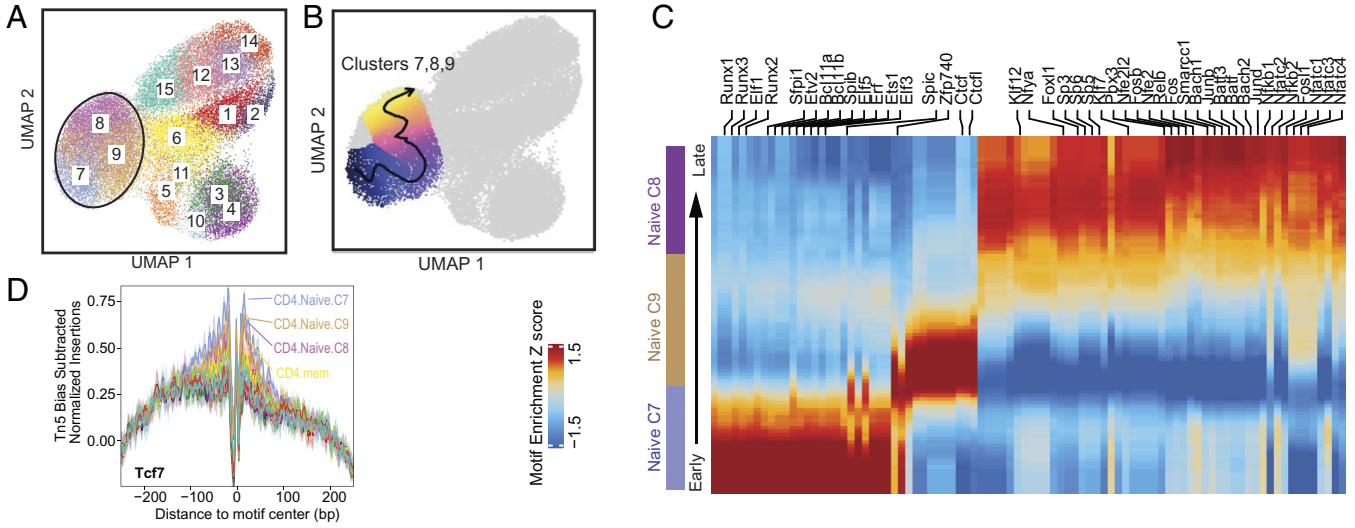

Fig. 5. CD4 NaiveT cell subsets fall along a developmental trajectory. (*A*) Further subclustering of CD4+ T cells reveals three naive cell populations. (*B*) Cell alignment to the pseudotime developmental trajectory within the naive CD4+ T cell populations. The smoothened arrow represents a visualization of the interpreted trajectory in the UMAP embedding. (*C*) Pseudotime heatmap ordering of the top 10% most variable chromVAR TF motif bias-corrected deviations in the CD4+ naive T cell trajectory. For *B*–*D*, n = 11,954 cells. (*D*) Tcf7 TFBS leaves a "deepest footprint" in a CD4+ naive cluster. Comparison of aggregate footprints for Tcf7 in CD4.naive, CD4.naiveIsgHi, CD4.naive Early Activation for mice of all four age groups. *Y*-axis values are average normalized reads per motif site, per mouse, at sites that are close with age.

Transcriptional and Epigenetic Programs Defining Age-Associated CD4$^+$ and CD8$^+$ Gzmk+ T Cells. Aging is marked by chronic low-grade inflammation, which contributes to tissue deterioration and the development of age-related diseases (64). Clonal cytotoxic Gzmk+ CD8+ T cells are recognized as a key feature of inflammaging in both mice and humans (21). Additionally, recent findings indicate that CD4+ T helper cells can also acquire cytotoxic properties, with Gzmk+ CD4+ T cells identified in aged mice (20).

Our scRNA-seq analysis identifies cytotoxic Gzmk+ CD4+ and Gzmk+ CD8+ T cells, which exhibit distinct features related to cytotoxic T cell development and function (Fig. 6*A*). These features include elevated expression of Gzmk, along with cytolytic and proinflammatory molecules such as Prf1, Gzma, Gzmb, and IFNγ. Additionally, Gzmk+ cells show increased expression of Cxcr3 and inflammatory chemokines Ccl5 and Ccl4 (Fig. 6*A*). Both Gzmk+ CD4+ and CD8+ T cell populations display the highest levels of Nkg7, which is critical for CD8+ T cell cytotoxicity and CD4+ T cell activation and proinflammatory responses (65).

Cytotoxic CD4+ T cell development is governed by a hierarchical transcriptional network involving the transcription factors ThPOK, Runx3, and Eomes (66–68). Specifically, Runx3 activation represses ThPOK, promoting a cytotoxic CD4+ T cell fate (43, 69). In CD8+ T cells, post-Lymphocytic Choriomeningitis Virus infection signatures reveal increased expression of Gzmk, Tox, and Eomes (70), indicating shared transcriptional programs that confer the Gzmk+ cytotoxic phenotype across both subsets. Notably, we observed elevated levels of Eomes and Runx3 in cytotoxic Gzmk+ CD4+ and CD8+ T cells (Fig. 6*A*).

Interestingly, we observed elevated expression levels of Tox, associated with T cell dysfunction, in the cytotoxic Gzmk+ CD8+ T cell population compared to CD8+ TEM cells (Fig. 6*A*). This finding aligns with the more dysfunctional phenotype seen in cells subjected to prolonged TCR activation during aging (71). Among CD4+ T cell subsets, Gzmk+ CD4+ T cells exhibited the highest Tox expression, surpassing that of CD4+ Dysfunctional and Activated Treg populations (Fig. 6*A*).

scATAC-seq data reveal cluster-specific increases in chromatin accessibility at the Eomes promoter (*SI Appendix*, Fig. S8), indicating transcriptional activation of Eomes in both Gzmk+ CD4+ and Gzmk+ CD8+ T cell populations. Additionally, footprint analysis of EOMES transcription factor binding sites across open chromatin regions shows the highest enrichment in cytotoxic CD4+ T and Th1 cells (Fig. 6*B*) compared to other CD4+ T cell subpopulations.

We assessed transcription factor activity across cells and clusters by weighting the presence of binding site motifs in open chromatin regions (Fig. 6*C* and *SI Appendix*, Fig. S8*B*). This analysis revealed an enrichment of Eomes binding site motifs in cytotoxic CD8+ T cells (*SI Appendix*, Fig. S8*C*), as well as in cytotoxic CD4+ T cells and effector memory and Th1 CD4+ T cells (Fig. 6*C*).

Motif enrichment analysis revealed subtype-specific activation of Tbx (Tbx1, Tbx2, Tbx4, Tbx5, Tbx10, Tbx20) and Runx (Runx1, Runx3) transcription factors in both Gzmk+ CD8+ and

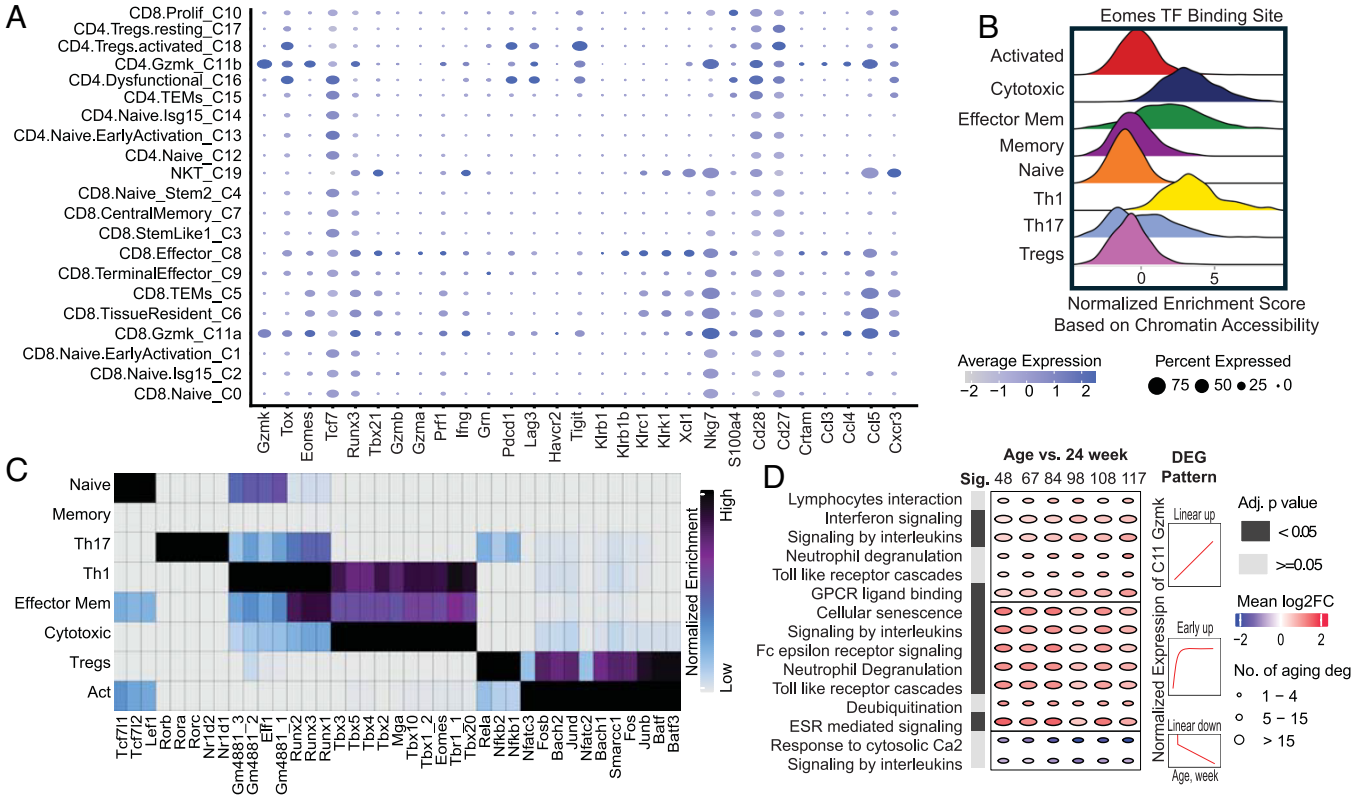

Fig. 6. Single-cell analysis of age-associated Gzmk$^+$ CD4$^+$ T cells and Gzmk$^+$ CD8$^+$ T cells. (*A*) scRNA-seq clusters of CD3+ T cells from spleens of C57BL/6 mice of 10 age groups (10 to 117 wk, n = 8 to 10 mice per age group). Dotplot of selected genes' average expression per cluster. (*B*) Normalized transcription factor enrichment profile for EOMES for all CD4+ T cell clusters in scATAC-seq. (*C*) Heatmap of transcription factors motifs enrichment scores of the most accessible genes in each scATAC-seq CD4+ T cell cluster. (*D*) Graphic representation of pathways enriched by differential age-related genes (aging DEG) for Gzmk+ T cell cluster–based pseudobulk across multiple ages (comparing samples from week 48 to week 117 to samples from week 24). Dark squares on the left indicate enrichment of a specific pathway was statistically significant. Each column of circles corresponds to the comparison between 24 wk and the older age. Circle size represents the number of age-related genes enriched to each pathway. The circle color indicates the average fold-change in the expression levels of these genes versus 24 wk, with the deepest red being an increase of ≥ four-fold. *Right* panels show the aging DEG patterns included in the pathway analysis in *Left* and *Middle* panels.

Gzmk+ CD4+ T cells (Fig. 6*C* and *SI Appendix*, Fig. S8*B*). This suggests a potential role for these regulators in mediating increased cytotoxic T cell activity and numbers with age.

We employed the methodologies outlined by ref. 72 to investigate age-related genes and pathways that emerge after the maturation of mice. Among all cell types analyzed, Gzmk+ T cells and CD8+ central memory T cells (CD8.TEM) exhibited the highest number of age-related genes (*SI Appendix*, Fig. S8*C*). In particular, age-related genes in Gzmk+ T cells were significantly enriched in multiple biological pathways compared to other subtypes of T cells (*SI Appendix*, Fig. S8*D*). Age-related genes enriched in pathways such as lymphocyte interactions with other cells and GPCR ligand binding demonstrated a linear increasing trend throughout aging (referred to as the "Linear Up Pattern") (Fig. 6*D*). In contrast, genes associated with pathways such as cellular senescence, Fcε receptor signaling, estrogen receptor signaling, neutrophil degranulation, and deubiquitination exhibited increased expression at earlier stages of life in mice (called the "early upward pattern") (Fig. 6*D*).

Furthermore, a different set of age-related genes involved in the response to elevated platelet cytosolic Ca2+ levels displayed a linear decrease in expression over time (designated the "linear down pattern") (Fig. 6*D*). Pathways such as IFN signaling and interleukin signaling showed enrichment with age-related genes in various patterns in Gzmk+ T cells, while also being enriched in other cell types (*SI Appendix*, Fig. S8*D*). This finding of IFN upregulation was also found in our previous work, in other tissues (72, 73).

These findings underscore significant transcriptional and epigenetic parallels between Gzmk+ CD4+ and Gzmk+ CD8+ T cells, implicating Eomes, Runx, Tox, and T-box in the development and function of these age-associated T cell subsets.

Discussion

Our findings align with previous research showing a decline in the population of naive T cells, alongside an increase in memory and effector T cells with age. Notably, recent studies have documented a decrease in naive CD8+ T cells and identified an age-associated CD8+ T cell subpopulation characterized by exhaustion markers and elevated Gzmk expression (21, 74). We confirm these findings but also identify distinct subsets, underscoring the robustness and sensitivity of our approach in detecting significant shifts in the immune landscape.

Orthogonal validation using flow cytometry confirmed the RNA-seq data, revealing a decrease in naive T cells and an increase in effector and memory T cells in aged mice. Additionally, the reduction in absolute CD4+ T cell numbers per gram of spleen in aged animals supports the notion of age-associated immune decline.

A key finding of our study is the characterization of the Gzmk+ T cell subpopulation. Gzmk, a serine protease involved in immune functions such as cytotoxicity and inflammation, showed a significant increase in aged mice, particularly within effector memory and exhausted T cell compartments. This suggests that Gzmk+ T cells may contribute to the age-related shift toward a proinflammatory and less effective immune response (74, 75). Our results therefore indicate that Gzmk+ T cells and Gzmk itself may serve as potential targets for addressing age-associated immune dysfunction. While aging activates the Gzmk pathway predominantly in cytotoxic CD4+ cells, specific antigens may induce different cytotoxic profiles. For instance, cytotoxic CD4+ T cells from CMV seropositive donors arise from Th1 precursors and utilize the perforin pathway (76, 77), whereas dengue virus–specific cytotoxic CD4+ T cells rely on Fas-FasL-mediated killing (78). Notably, allograft rejection by cytotoxic CD4+ T cells appears to involve both perforin and Fas-FasL mechanisms (79).

Heterogeneity in chemokine gene expression among cytotoxic T cells may reflect functional diversity linked to specific antigens. For example, two distinct subsets of cytotoxic CD4+T cells identified during CMV infection shared many TCR repertoires but differed in chemokine expression (CCL5 versus CCL3 and CCL4) (80).

Among age-related gene perturbations, we noted significant upregulation of ISG15 in older T cell populations. This IFN-stimulated gene indicates increased IFN signaling consistent with a proinflammatory phenotype, corroborated by prior studies in other tissues (73, 81). It is suggested that age-related increases in IFN signaling stem from a loss of heterochromatin, leading to heightened transcription of repetitive DNA elements like LINE-1 (82).

Additional age-related genes include TNFRSF4 and TNFRSF9, which activate NF-κB signaling (83), further indicating increased inflammatory signaling. The scATAC-seq data provided additional layers of information by revealing changes in chromatin accessibility associated with aging. For instance, the increase accessibility of promoters for genes like IL-17α and RORγ in aged mice also suggests a shift toward a more proinflammatory T cell phenotype, which has been implicated in age-related chronic inflammation and autoimmunity (58, 59).

The scATAC-seq data from this study revealed changes in chromatin accessibility associated with aging. Increased accessibility of promoters for genes such as IL-17α and RORγ suggests a shift toward a proinflammatory T cell phenotype implicated in age-related chronic inflammation and autoimmunity (58, 59). We also identified transcription factors like EOMES, RUNX, TOX, and T-BOX as key regulators of age-associated changes in T cell subsets. The enrichment of Eomesodermin Eomes binding sites in cytotoxic CD4+ is congruent with the central role of this T-box transcription factor in the development and function of cytotoxic T cell populations (68, 84–86). Similarly, the prominent increase in Eomes binding sites in accessible chromatin regions observed in effector memory T cells is consistent with the combined requirement of Eomes and Tbet, a related T-box factor, in the development of antitumor cytotoxic effector/central memory T cells (87).

Future research should be aimed at determining whether these findings are predictive of changes observed in aged human beings and exploring the functional consequences of targeting these pathways in the setting of age-related immune dysfunction.

Materials and Methods

Mice and Sample Processing. Wild-type male C57BL/6 mice were obtained from The Jackson Laboratory and housed under pathogen-free conditions at Regeneron, following Institutional Animal Care and Use Committee guidelines. For scRNA-seq, T cells were collected from spleens across 10 age groups. For scATAC-seq, nuclei were isolated from spleens across 4 age groups.

Preparation and Sequencing of scRNA-seq and TCR Library. Single-cell suspensions were processed for droplet-based scRNA-seq using the 10× Genomics platform. Cells were loaded onto a Chromium Single Cell Instrument to generate GEM droplets, with libraries prepared using the Chromium Single Cell 3′ and 5′ Library Kits. TCR α/β libraries were amplified with in-house primers and sequenced on an Illumina NextSeq500. Data preprocessing utilized the Cell Ranger Suite v2.0 for demultiplexing, UMI counting, and alignment to the mouse mm10 genome.

Preparation and Sequencing of scATAC-seq Library. Nuclei were prepared using the 10× Genomics protocol and processed on a Chromium Single Cell Instrument with the NextGEM ATAC-seq v1.1 assay. Libraries were sequenced on an Illumina NextSeq500, with data preprocessed using Cell Ranger ATAC v1.0 aligned to the GRCm38 genome.

Experimental Validation. For flow cytometry, purified splenic CD3+ T cells were stimulated for 48 h, stained with viability dye and primary antibodies, followed by intracellular labeling. CD8+ T cells from young and aged mice were isolated and activated with anti-CD3/CD28 antibodies and IL-2 for cytokine analysis via flow cytometry. Supernatants were collected for ELISA measurements of Granzyme B, CCL3/MIP-1α, CCL4/MIP-1β, and CCL5/RANTES.

scRNA-seq Data Processing and Analysis. Quality control. scRNA-seq data from 83 mice across 10 ages were filtered using Scanpy (v.1.4.6) based on UMI counts, gene detection ratios, and mitochondrial gene expression. After normalization and Principal Component Analysis clustering with the Leiden algorithm, batch correction was performed using Harmony, retaining 28,187 of 30,163 cells (96.7%).

Clustering and Analysis. T cells were identified by TCR beta chain sequences. Clustering was performed at resolutions from 0.5 to 2, with a resolution of 1.0 selected based on marker gene representation, resulting in 25 unsupervised clusters. Cluster annotations utilized Differential Expression Genes (DEGs) and enrichment of T cell gene signatures. DEGs were calculated using recommended parameters, and subclustering of naive T cells and Treg populations was conducted via Wilcoxon tests for top DEGs. Uniform ManifoldApproximation and Projection (UMAP) was employed for dimensionality reduction. The top 10 overexpressed genes per cluster were selected based on Wilcoxon test results ($P < 0.05$, Log2 Fold Change < 1). All CD3D+/CD3E+ clusters were retained for further analysis, resulting in a total of 260,872 cells.

Age Relating Pathway Enrichment Analysis. Methods from ref. 72 were used to identify age-related genes after combining single cells from each mouse for each cell type. REACTOME pathways were used for the pathway enrichment.

Paired scTCRα/TCRβ Repertoire Analysis. Sample demultiplexing and barcode processing were conducted using the Cell Ranger Single-Cell Software Suite, with alignment and TCR assembly performed by Cell Ranger VDJ v3.0.2. Only TCRs with one productive rearrangement for both TCRα and TCRβ chains were included. Clonotype frequencies were calculated, and Gini coefficients assessed repertoire diversity and clonality. TCR clonotypes were defined by the gene combination and nucleotide sequence of the CDR3 region. Cell counts per cluster were obtained using scRepertoire, and TCR data were cross-referenced with public datasets from VDJdb.

scATAC-seq Data Processing and Analysis. Quality control. Aligned reads from Cell Ranger were preprocessed to retain high-quality reads and remove PCR duplicates. We adjusted mapping for scATAC-seq and performed barcode filtering based on fragment count and promoter ratios. A two-step genome accessibility-based clustering identified high-quality T cells: The first step used unbiased methods for peak calling, while the second refined clusters to isolate CD4+ and CD8+ T cells.

Clustering and Annotation. CD4+ and CD8+ T cell clusters were analyzed separately using ArchR v.1.0.1 (88). Harmony was employed for batch correction, and Seurat clustering was applied to CD8+ T cells at a resolution of 0.6, yielding nine clusters. Clusters were annotated by integrating scRNA-seq data from the same mice, with MACS2 used for peak calling in each CD8+ cluster. A similar approach identified 15 refined clusters among CD4+ T cells.

Gene Activity Score. Gene activity scores were computed by integrating ATAC-seq signals from annotated gene bodies, −5 kb upstream of transcription start sites, and +10 kb downstream of transcription termination sites. Spearman correlation between ATAC-seq gene scores and RNA-seq expression was calculated to align scATAC-seq and scRNA-seq clusters.

TF Motif Enrichment. TF motif enrichment in each cell cluster was assessed using chromVAR (89). We collected Catalog of Inferred Sequence Binding Preferencesmotifs for 857 TFs (Transcription Factors) and calculated GC bias-corrected deviation scores and variability for each motif.

Pseudotime Analysis. Cells from naive clusters were ordered in pseudotime, with changes in gene scores and TF motifs visualized along the trajectory using heatmaps in ArchR.

Public scATAC-seq Signature. ATAC-seq peak and signal data were obtained from Yoshida et al. (90). We calculated the average accessibility of all peaks for each cluster and identified 162,559 shared peaks by overlapping our data with that of Yoshida et al. Spearman correlation of average accessibility was then computed across all clusters.

Data, Materials, and Software Availability. Raw single-cell RNA-sequencing TCR-sequencing and ATAC sequencing data have been deposited in Sequence Read Archive at the National Center for Biotechnology Information (PRJNA1181768)(91).

ACKNOWLEDGMENTS. We thank George Yancopoulos, Len Schleifer, Drew Murphy, and the rest of the Regeneron community for their support. We would like to thank Donna Hylton for assistance with cytokines measurements by Enzyme-linked immunosorbent assay. Yueming Ding, and Lance Zhang ran the single-cell data preprocessing pipeline, and Samvitha Cherravuru helped in single-cell lab work. We thank William Palmer, Jessie Brown, and Jose Rodriguez Cortes for manuscript feedback.

1. Z. Liu *et al.*, Immunosenescence: Molecular mechanisms and diseases. *Signal Transduct. Target. Ther.* **8**, 200 (2023).
2. J. J. Goronzy, C. M. Weyand, Immune aging and autoimmunity. *Cell. Mol. Life Sci.* **69**, 1615 (2012).
3. J. B. Mannick, D. W. Lamming, Targeting the biology of aging with mtor inhibitors. *Nat. Aging* **3**, 642–660 (2023).
4. V. Panwar *et al.*, Multifaceted role of mtor (mammalian target of rapamycin) signaling pathway in human health and disease. *Signal Transduct. Target. Ther.* **8**, 375 (2023).
5. A. Ortega-Molina *et al.*, A mild increase in nutrient signaling to mtorc1 in mice leads to parenchymal damage, myeloid inflammation and shortened lifespan. *Nat. Aging* **4**, 1102–1120 (2024).
6. J. B. Mannick *et al.*, mtor inhibition improves immune function in the elderly. *Sci. Transl. Med.* **6**, 268ra179 (2014).
7. J. J. Young *et al.*, Aging gene signature of memory cd8+ t cells is associated with neurocognitive functioning in alzheimer's disease. *Immun. Ageing* **20**, 71 (2023).
8. K. Y. Yang *et al.*, Single-cell transcriptomics of treg reveals hallmarks and trajectories of immunological aging. *J. Leukoc. Biol.* **115**, 19–35 (2024).
9. R. I. Martínez-Zamudio *et al.*, Senescence-associated β-galactosidase reveals the abundance of senescent cd8+ t cells in aging humans. *Aging Cell* **20**, e13344 (2021).
10. D. K. Pieren, N. A. Smits, M. D. van de Garde, T. Guichelaar, Response kinetics reveal novel features of ageing in murine t cells. *Sci. Rep.* **9**, 5587 (2019).
11. N. Minato, M. Hattori, Y. Hamazaki, Physiology and pathology of t-cell aging. *Int. Immunol.* **32**, 223–231 (2020).
12. H. Mkhikian *et al.*, Age-associated impairment of t cell immunity is linked to sex-dimorphic elevation of n-glycan branching. *Nat. Aging* **2**, 231–242 (2022).
13. T. Mi *et al.*, Conserved epigenetic hallmarks of t cell aging during immunity and malignancy. *Nat. Aging* **4**, 1053–1063 (2024).
14. J. J. Goronzy, C. M. Weyand, Successful and maladaptive t cell aging. *Immunity* **46**, 364–378 (2017).
15. L. Haynes, A. C. Maue, Effects of aging on t cell function. *Curr. Opin. Immunol.* **21**, 414 (2009).
16. R. Elias, T. Karantanos, E. Sira, K. L. Hartshorn, Immunotherapy comes of age: Immune aging & checkpoint inhibitors. *J. Geriatr. Oncol.* **8**, 229–235 (2017).
17. J. Nikolich-Žugich, The twilight of immunity: Emerging concepts in aging of the immune system. *Nat. Immunol.* **19**, 10–19 (2017).
18. E. Montecino-Rodriguez, B. Berent-Maoz, K. Dorshkind, Causes, consequences, and reversal of immune system aging. *J. Clin. Invest.* **123**, 958–965 (2013).
19. I. den Braber *et al.*, Maintenance of peripheral naive t cells is sustained by thymus output in mice but not humans. *Immunity* **36**, 288–297 (2012).
20. Y. Elyahu *et al.*, Aging promotes reorganization of the cd4 t cell landscape toward extreme regulatory and effector phenotypes. *Sci. Adv.* **5**, eaaw8330 (2019).
21. D. A. Mogilenko *et al.*, Comprehensive profiling of an aging immune system reveals clonal gzmk+ cd8+ t cells as conserved hallmark of inflammaging. *Immunity* **54**, 99–115.e12 (2021).
22. M. Terekhova *et al.*, Single-cell atlas of healthy human blood unveils age-related loss of nkg2c+ gzmb- cd8+ memory t cells and accumulation of type 2 memory t cells. *Immunity* **56**, 2836–2854 (2023).
23. X. Shen *et al.*, Nonlinear dynamics of multi-omics profiles during human aging. *Nat. Aging* **1**, 1619–1634 (2024).
24. G. X. Zheng *et al.*, Massively parallel digital transcriptional profiling of single cells. *Nat. Commun.* **8**, 14049 (2017).
25. A. Butler, P. Hoffman, P. Smibert, E. Papalexi, R. Satija, Integrating single-cell transcriptomic data across different conditions, technologies, and species. *Nat. Biotechnol.* **36**, 411–420 (2018).
26. F. A. Wolf, P. Angerer, F. J. Theis, Scanpy: Large-scale single-cell gene expression data analysis. *Genome Biol.* **19**, 15 (2018).
27. M. Andreatta *et al.*, Interpretation of t cell states from single-cell transcriptomics data using reference atlases. *Nat. Commun.* **12**, 2965 (2021).
28. N. Palau *et al.*, Genome-wide transcriptional analysis of t cell activation reveals differential gene expression associated with psoriasis. *BMC Genomics* **14**, 825 (2013).
29. E. Sebzda, Z. Zou, J. S. Lee, T. Wang, M. L. Kahn, Transcription factor klf2 regulates the migration of naive t cells by restricting chemokine receptor expression patterns. *Nat. Immunol.* **9**, 292–300 (2008).

30. J. P. Hewitson *et al.*, Malat1 suppresses immunity to infection through promoting expression of maf and il-10 in th cells. *J. Immunol.* **204**, 2949–2960 (2020).
31. D. Ucar *et al.*, The chromatin accessibility signature of human immune aging stems from cd8+ t cells. *J. Exp. Med.* **214**, 3123–3144 (2017).
32. P. A. Szabo *et al.*, Single-cell transcriptomics of human t cells reveals tissue and activation signatures in health and disease. *Nat. Commun.* **10**, 4706 (2019).
33. V. Iglesias-Guimarais *et al.*, Ifn-stimulated gene 15 is an alarmin that boosts the ctl response via an innate, nk cell–dependent route. *J. Immunol.* **204**, 2110–2121 (2020).
34. G. Escobar, D. Mangani, A. C. Anderson, T cell factor 1: A master regulator of the t cell response in disease. *Sci. Immunol.* **5**, 9726 (2020).
35. E. M. Steinert *et al.*, Quantifying memory cd8 t cells reveals regionalization of immunosurveillance. *Cell* **161**, 737–749 (2015).
36. L. R. Shiow *et al.*, Cd69 acts downstream of interferon-α/β to inhibit s1p1 and lymphocyte egress from lymphoid organs. *Nature* **440**, 540–544 (2006).
37. B. C. Miller *et al.*, Subsets of exhausted cd8+ t cells differentially mediate tumor control and respond to checkpoint blockade. *Nat. Immunol.* **20**, 326–336 (2019).
38. S. Sarkar *et al.*, Functional and genomic profiling of effector cd8 t cell subsets with distinct memory fates. *J. Exp. Med.* **205**, 625–640 (2008).
39. D. Zemmour *et al.*, Single-cell gene expression reveals a landscape of regulatory t cell phenotypes shaped by the tcr. *Nat. Immunol.* **19**, 291–301 (2018).
40. N. R. Cunningham *et al.*, Immature cd4+cd8+ thymocytes and mature t cells regulate nur77 distinctly in response to tcr stimulation. *J. Immunol.* **177**, 6660–6666 (2006).
41. N. P. Weng, Y. Araki, K. Subedi, The molecular basis of the memory t cell response: Differential gene expression and its epigenetic regulation. *Nat. Rev. Immunol.* **12**, 306–315 (2012).
42. N. Chihara *et al.*, Induction and transcriptional regulation of the co-inhibitory gene module in t cells. *Nature* **558**, 454–459 (2018).
43. D. Mucida *et al.*, Transcriptional reprogramming of mature cd4+ helper t cells generates distinct mhc class ii–restricted cytotoxic t lymphocytes. *Nat. Immunol.* **14**, 281–289 (2013).
44. J. A. Juno *et al.*, Cytotoxic cd4 t cells–friend or foe during viral infection? *Front. Immunol.* **8**, 242741 (2017).
45. M. Xie, J. Wei, J. Xu, Inducers, attractors and modulators of cd4+ treg cells in non-small-cell lung cancer. *Front. Immunol.* **11**, 522557 (2020).
46. M. Hinterbrandner *et al.*, Tnfrsf4-expressing regulatory t cells promote immune escape of chronic myeloid leukemia stem cells. *JCI Insight* **6**, e151797 (2021).
47. K. Naylor *et al.*, The influence of age on t cell generation and tcr diversity. *J. Immunol.* **174**, 7446–7452 (2005).
48. M. Ahmed *et al.*, Clonal expansions and loss of receptor diversity in the naive cd8 t cell repertoire of aged mice. *J. Immunol.* **182**, 784–792 (2009).
49. V. Decman *et al.*, Defective cd8 t cell responses in aged mice are due to quantitative and qualitative changes in virus-specific precursors. *J. Immunol.* **188**, 1933–1941 (2012).
50. J. F. Miller, The function of the thymus and its impact on modern medicine. *Science* **369**, eaba2429 (2020).
51. Y. Elyahu, A. Monsonego, Thymus involution sets the clock of the aging t-cell landscape: Implications for declined immunity and tissue repair. *Ageing Res. Rev.* **65**, 101231 (2021).
52. J. S. Sutherland *et al.*, Activation of thymic regeneration in mice and humans following androgen blockade. *J. Immunol.* **175**, 2741–2753 (2005).
53. J. Baran-Gale *et al.*, Ageing compromises mouse thymus function and remodels epithelial cell differentiation. *Elife* **9**, e56221 (2020).
54. J. Dooley, A. Liston, Molecular control over thymic involution: From cytokines and microrna to aging and adipose tissue. *Eur. J. Immunol.* **42**, 1073–1079 (2012).
55. D. H. Gray *et al.*, Developmental kinetics, turnover, and stimulatory capacity of thymic epithelial cells. *Blood* **108**, 3777–3785 (2006).
56. J. C. Kimmel *et al.*, Murine single-cell rna-seq reveals cell-identity- and tissue-specific trajectories of aging. *Genome Res.* **29**, 2088–2103 (2019).
57. N. Almanzar *et al.*, A single-cell transcriptomic atlas characterizes ageing tissues in the mouse. *Nature* **583**, 590–595 (2020).
58. G. Huang, Y. Wang, H. Chi, Regulation of th17 cell differentiation by innate immune signals. *Cell. Mol. Immunol.* **9**, 287–295 (2012).
59. M. A. Lim *et al.*, Increased th17 differentiation in aged mice is significantly associated with high il-1β level and low il-2 expression. *Exp. Gerontol.* **49**, 55–62 (2014).
60. Y. Zhong *et al.*, Hierarchical regulation of the resting and activated t cell epigenome by major transcription factor families. *Nat. Immunol.* **23**, 122–134 (2021).
61. D. Pham *et al.*, Batf pioneers the reorganization of chromatin in developing effector t cells via ets1-dependent recruitment of ctcf. *Cell Rep.* **29**, 1203–1220.e7 (2019).
62. T. Lawrence, The nuclear factor nf-κb pathway in inflammation. *Cold Spring Harb. Perspect. Biol.* **1**, a001651 (2009).
63. T. Hofland *et al.*, Cd4+ t cell memory is impaired by species-specific cytotoxic differentiation, but not by tcf-1 loss. *Front. Immunol.* **14**, 1168125 (2023).
64. C. Franceschi, P. Garagnani, P. Parini, C. Giuliani, A. Santoro, Inflammaging: A new immune–metabolic viewpoint for age-related diseases. *Nat. Rev. Endocrinol.* **14**, 576–590 (2018).
65. S. S. Ng *et al.*, The nk cell granule protein nkg7 regulates cytotoxic granule exocytosis and inflammation. *Nat. Immunol.* **21**, 1205–1218 (2020).
66. H. Cheroutre, M. M. Husain, Cd4 ctl: Living up to the challenge. *Semin. Immunol.* **25**, 273–281 (2013).
67. J. Zhu, H. Yamane, W. E. Paul, Differentiation of effector cd4+ t cell populations. *Annu. Rev. Immunol.* **28**, 445–489 (2010).
68. E. L. Pearce *et al.*, Control of effector cd8+ t cell function by the transcription factor eomesodermin. *Science* **302**, 1041–1043 (2003).
69. B. S. Reis, A. Rogoz, F. A. Costa-Pinto, I. Taniuchi, D. Mucida, Mutual expression of the transcription factors runx3 and thpok regulates intestinal cd4+ t cell immunity. *Nat. Immunol.* **14**, 271–279 (2013).
70. I. Sandu *et al.*, Landscape of exhausted virus-specific cd8 t cells in chronic lcmv infection. *Cell Rep.* **32**, 108078 (2020).
71. O. Khan *et al.*, Tox transcriptionally and epigenetically programs cd8+ t cell exhaustion. *Nature* **571**, 211–218 (2019).
72. T. Shavlakadze *et al.*, Age-related gene expression signatures from limb skeletal muscles and the diaphragm in mice and rats reveal common and species-specific changes. *Skelet. Muscle* **13**, 11 (2023).
73. T. Shavlakadze *et al.*, Age-related gene expression signature in rats demonstrate early, late, and linear transcriptional changes from multiple tissues. *Cell Rep.* **28**, 3263–3273.e3 (2019).
74. S. J. Han, P. Georgiev, A. E. Ringel, A. H. Sharpe, M. C. Haigis, Age-associated remodeling of t cell immunity and metabolism. *Cell Metab.* **35**, 36–55 (2023).
75. A. Jain, I. Sturmlechner, C. M. Weyand, J. J. Goronzy, Heterogeneity of memory t cells in aging. *Front. Immunol.* **14**, 1250916 (2023).
76. N. B. Marshall, S. L. Swain, Cytotoxic cd4 t cells in antiviral immunity. *Biomed Res. Int.* **2011**, 954602 (2011).
77. Y. Serroukh *et al.*, The transcription factors runx3 and thpok cross-regulate acquisition of cytotoxic function by human th1 lymphocytes. *Elife* **7**, e30496 (2018).
78. Y. Tian, A. Sette, D. Weiskopf, Cytotoxic cd4 t cells: Differentiation, function, and application to dengue virus infection. *Front. Immunol.* **7**, 232069 (2016).
79. T. J. Grazia *et al.*, Acute cardiac allograft rejection by directly cytotoxic cd4 t cells: Parallel requirements for fas and perforin. *Transplantation* **89**, 33–39 (2010).
80. M. Lyu *et al.*, Dissecting the landscape of activated cmv-stimulated cd4+ t cells in humans by linking single-cell rna-seq with t-cell receptor sequencing. *Front. Immunol.* **12**, 779961 (2021).
81. T. Shavlakadze *et al.*, Short-term low-dose mtorc1 inhibition in aged rats counter-regulates age-related gene changes and blocks age-related kidney pathology. *J. Gerontol. A Biol. Sci. Med. Sci.* **73**, 845–852 (2018).
82. M. De Cecco *et al.*, Line-1 derepression in senescent cells triggers interferon and inflammaging. *Nature* **566**, 73 (2019).
83. T. Liu, L. Zhang, D. Joo, S. C. Sun, Nf-κb signaling in inflammation. *Signal Transduct. Target. Ther.* **2**, 17023 (2017).
84. S. M. Kaech, W. Cui, Transcriptional control of effector and memory cd8+ t cell differentiation. *Nat. Rev. Immunol.* **12**, 749–761 (2012).
85. H. Z. Qui *et al.*, Cd134 plus cd137 dual costimulation induces eomesodermin in cd4 t cells to program cytotoxic th1 differentiation. *J. Immunol.* **187**, 3555–3564 (2011).
86. M. A. Curran *et al.*, Systemic 4–1bb activation induces a novel t cell phenotype driven by high expression of eomesodermin. *J. Exp. Med.* **210**, 743–755 (2013).
87. G. Li *et al.*, T-bet and eomes regulate the balance between the effector/central memory t cells versus memory stem like t cells. *PLoS One* **8**, e67401 (2013).
88. J. M. Granja *et al.*, Archr is a scalable software package for integrative single-cell chromatin accessibility analysis. *Nat. Genet.* **53**, 403–411 (2021).
89. A. N. Schep, B. Wu, J. D. Buenrostro, W. J. Greenleaf, Chromvar: Inferring transcription-factor-associated accessibility from single-cell epigenomic data. *Nat. Methods* **14**, 975–978 (2017).
90. H. Yoshida *et al.*, The cis-regulatory atlas of the mouse immune system. *Cell* **176**, 897–912.e20 (2019).
91. J. He *et al.*, Single cell–resolved cellular, transcriptional and epigenetic changes in T cell populations linked to age-associated immune decline. NCBI BioProject. https://www.ncbi.nlm.nih.gov/bioproject/?term=PRJNA1181768=PRJNA1181768. Deposited 23 October 2024.